Supporting Information

A platinum-dithiolene monoanionic salt exhibiting multi-properties, including room-temperature proton-dependent solution luminescence

Salahuddin Attar, Davide Espa, Flavia Artizzu, M. Laura Mercuri,Angela Serpe, Elisa Sessini, Giorgio Concas, Francesco Congiu, Luciano Marchiò, Paola Deplano

Molecular Structure and MOs calculations

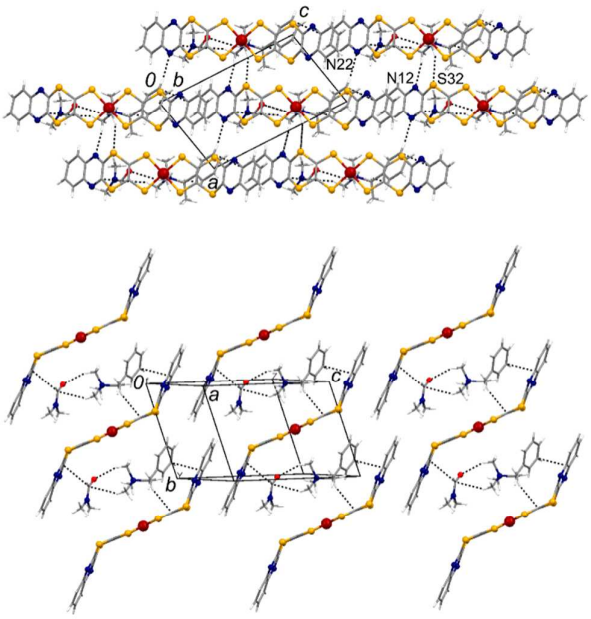

Figure S1. Crystal packing of (*R*)-Ph(Me)HC*-$NMe_3[PtL_2]$·DMF. Above, projection along the *b* axis. Below, projection approximately along the *a* axis. A portion of a supramolecular layer is shown. Dashed lines represent shortest contacts between the anion complex, DMF and the chiral cation.

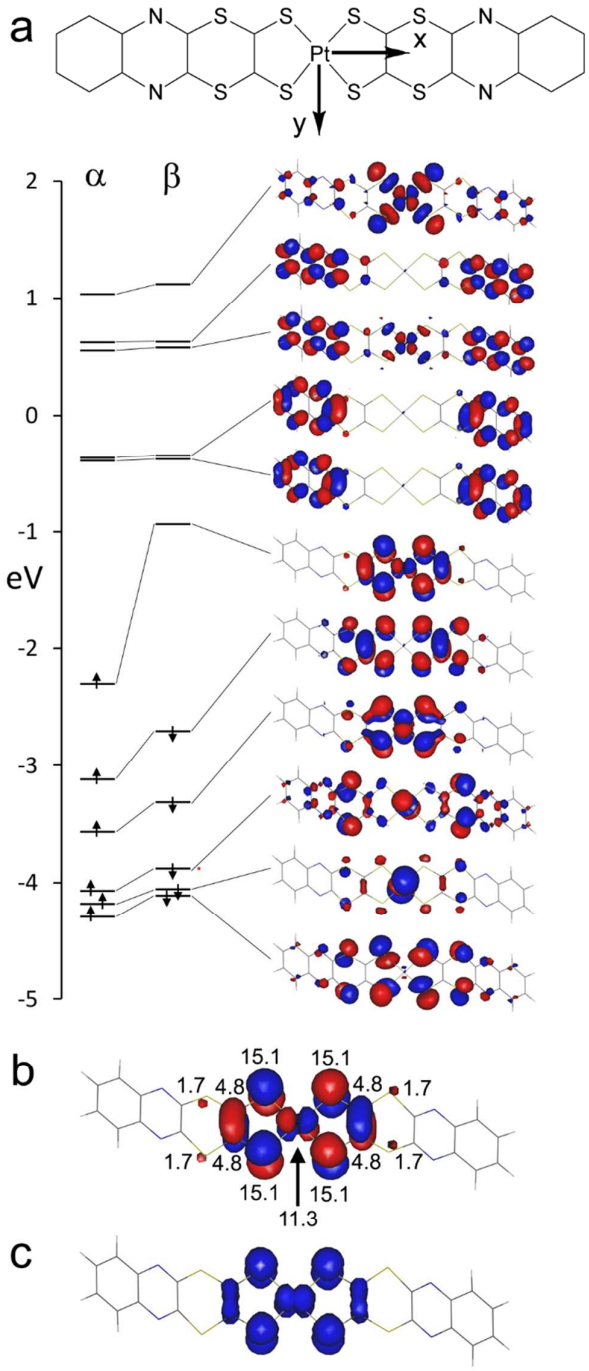

Figure S2. (a) Energy levels and Kohn-Sham molecular orbitals (MOs) for $[PtL_2]^-$ from a spin unrestricted calculation. (b) Percentage contributions of different atoms to the alpha SOMO of $[ML_2]^-$. (c) Depiction of the spin density distribution of $[PtL_2]^-$, isosurface plot at 0.001 esu $Å^{-3}$. B3LYP/def2-TZVP_6-311+G(d)

Magnetic Properties

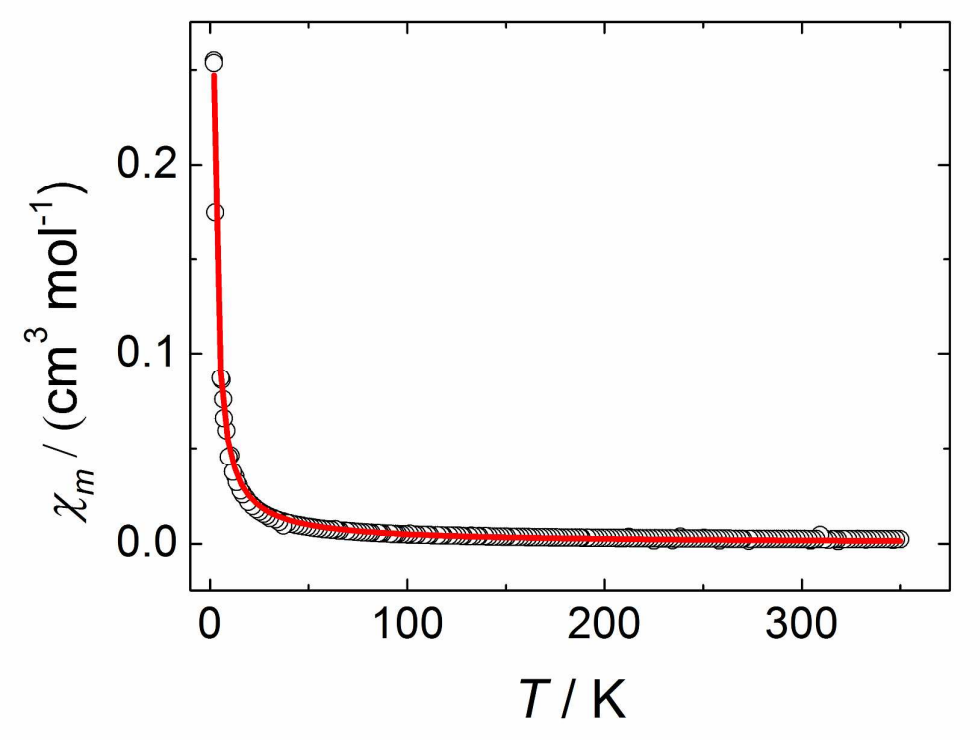

Figure S3. Molar magnetic susceptibility (CGS units) vs. temperature. Experimental data (open circles) and the fit curve (solid line) are shown.

DC magnetic susceptibility measurements on a polycrystalline sample of (*R*)-Ph(Me)HC*-$NMe_3[PtL_2]$·DMF were performed with a Quantum Design MPMS-XL-5 SQUID magnetometer in the temperature range 2–350 K. The molar magnetic susceptibility (CGS units) vs. temperature is shown in Figure S3. The temperature dependence of the susceptibility is well described by the Curie law:[i]

$$\chi_m = \frac{N\, p^2 \mu_B^2}{3kT}$$

Where N is the number of magnetic ions in a mole, $p = g[S(S+1)]^{1/2}$ is the effective Bohr magneton number, μ_B is the Bohr magneton and k is the Boltzmann constant. The fit gives an effective Bohr magneton number $p = 2.0 \pm 0.1$; the closest theoretical value is $p = 1.73$, corresponding to S=1/2. The good fit with a simple Curie law and the value of p suggest a magnetic behaviour typical of an

uncoupled *S*=1/2 ground state species.

According to the structural analysis, the presence of a partial π-stack through the peripheral aromatic fragment of the ligands (3.45(4) Å) may result in magnetic interactions, as observed in d^8-monoanionic bisdithiolene complexes. For example, it was found that a separation of 3.45(4) Å between neighbouring fragments in a nickel-bisdithiolene system causes strong antiferromagnetic interactions[i]. In the present case, stacking motifs are not favourable to induce magnetic interactions, and this can be easily explained by considering that the stacking occurs through the periphery of the ligand (see Figure 2 in the main text). In fact, the presence of a dithiino ring interposed between the aromatic moieties interrupts the communication with the metal-thiolate systems experiencing a spin density accumulation.

Optical properties

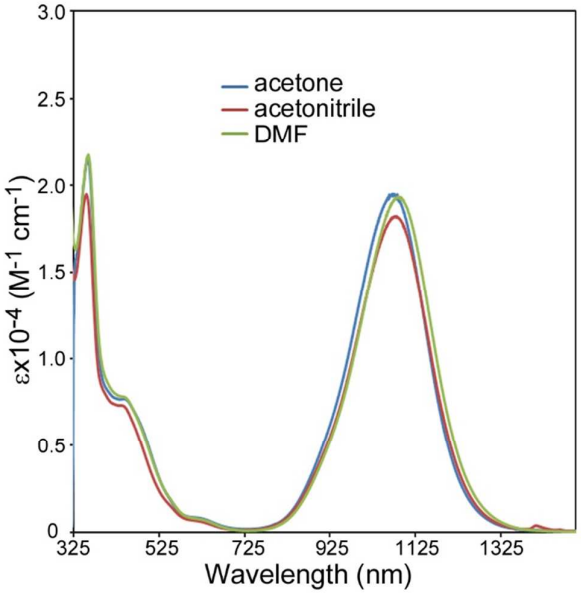

Figure S4. Absorption spectra for **1** in different solvents (Acetone, acetonitrile and DMF).

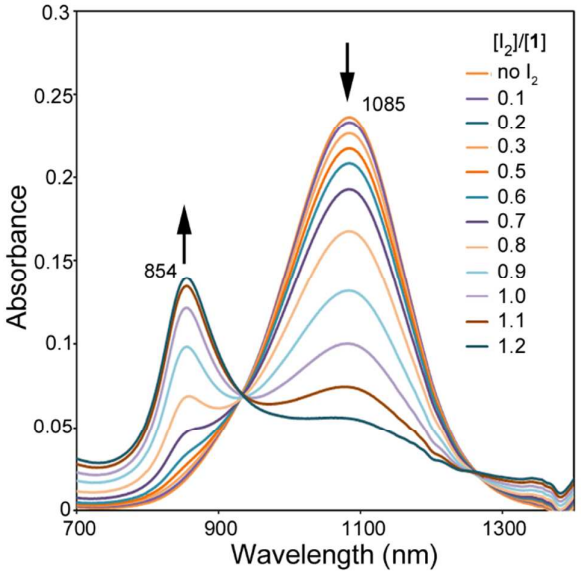

Figure S5. Changes of absorption spectra for **1** in DMF ($1.25 \cdot 10^{-5}$ M) on increasing concentrations of I_2. The new peak at 854 nm is ascribed to the formation of the neutral derivative. It should be remarked that the absorbance increase of the neutral species exhibits deviations from Beer's law which can be consistent with auto-association of the formed species.

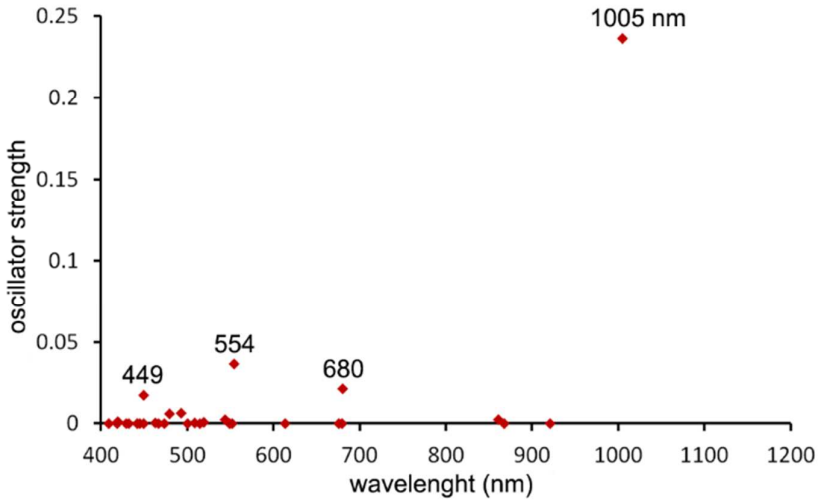

Figure S6. Oscillator strengths of the 30 excitations for **1** resulting from TD-DFT calculations.

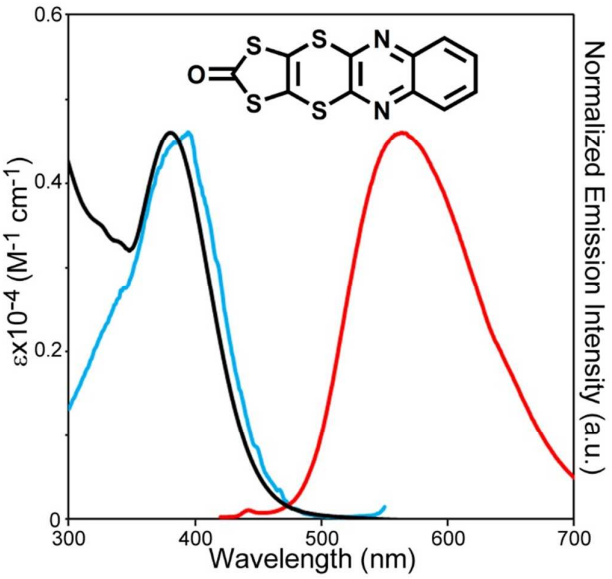

Figure S7. Absorption (black), emission (red) and excitation (blue) spectra of quinoxdt ligand (in the inset). Excitation wavelength was 390nm. Excitation spectrum was acquired by monitoring emission at 560 nm.

Photophysical parameters evaluation

Quantum yield

Emission quantum yield was evaluated using the relative method [ii] though the following equation:

$$\Phi = \Phi_R \frac{a_R}{a} \frac{I}{I_R} \frac{n^2}{n_R^2}$$

where the R index refers to the photoluminescence standard, Φ_R= reference quantum yield; $a_R=1-10^{-AR}$, absorption factor of the reference at excitation wavelength; $a=1-10^{-A}$, absorption factor of the sample at excitation wavelength; A_R=absorbance of the reference at excitation wavelength; A=absorbance of the sample at excitation wavelength; I=sample integrated emission; I_R=reference integrated emission; n = refractive index of the medium.

Table S1 For $[Ru(bpy)_3]^{2+}$: Excitation wavelength, λ_{exc}=450 nm. Emission maximum, λ_{max} = 610 nm. Concentration was $1.17\cdot10^{-5}$ M in water. For $[PtL_2]^-$: Excitation wavelength, λ_{exc}=420 nm. Emission maximum, λ_{max} = 566 nm (acetone), 572 nm (DMF). Concentration was $1.00\cdot10^{-4}$ M in acetone or DMF.

	A	$a=1-10^{-A}$	I	n	solvent	Φ
$Ru(bpy)_3^{2+}$	0.16	0.308169	$6.69\cdot10^8$	1.333	H_2O	0.063[ii]
$[PtL_2]^-$	0.91	0.878101	$1.97\cdot10^7$	1.36	acetone	0.0011
$[PtL_2]^-$	0.70	0.801948	$1.48\cdot10^7$	1.4305	DMF	0.0019

Estimated emission lifetime

The emission lifetime ($\tau_{obs} = 1/\kappa_{obs}$) of **1** was roughly estimated through the equation:

$$\Phi = \frac{\kappa_{rad}}{\kappa_{obs}}$$

where κ_{rad} is the rate constant for spontaneous emission, which in turn was estimated through the Strickler-Berg equation[iii]:

$$\kappa_{\mathrm{rad}} = \tau_{\mathrm{rad}}^{-1} = 8\pi n^2 c \frac{1}{\langle\lambda^3\rangle} \frac{g}{g'} \int \frac{\sigma(\lambda)}{\lambda} d\lambda$$

where *n* is the refractive index of the medium (1.43 for DMF), *c* is the speed of light in vacuum and *g*, *g'* refer to the degeneration of the ground and excited state respectively.$\langle\lambda^3\rangle$refers to the mean value of emission wavelength. $\sigma(\lambda)$ is the absorption cross-section of **1**, which was estimated through the excitation spectrum normalized to absorption. The estimated value of emission lifetime for **1** is 45 ps.

Proton quenching

The emission quenching of **1** upon proton addition was evaluated through the following equation:

$$\frac{I_0}{I_r} = 1 + K[\mathbf{H}^+]$$

where I_0, I_r represent the emission intensity in the absence and in the presence of the quencher ($\mathbf{H}^+$), respectively, while *K* is the constant of the quenching process.

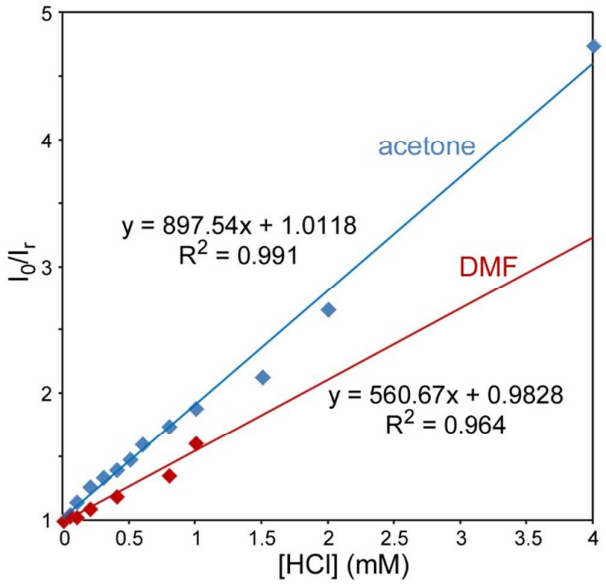

Figure S8. I_0/I_r vs. quencher concentration plot for the emission quenching of **1** by HCl addition in acetone (blue) and DMF (red). Dots represents experimental I_0/I_r values, solid lines represent linear fit to data.

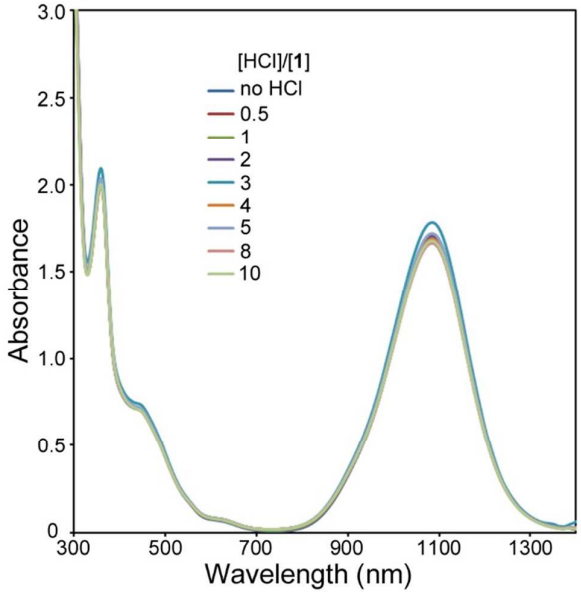

Figure S9. Absorption spectra for **1** in DMF solution on addition of increasing amount of HCl.

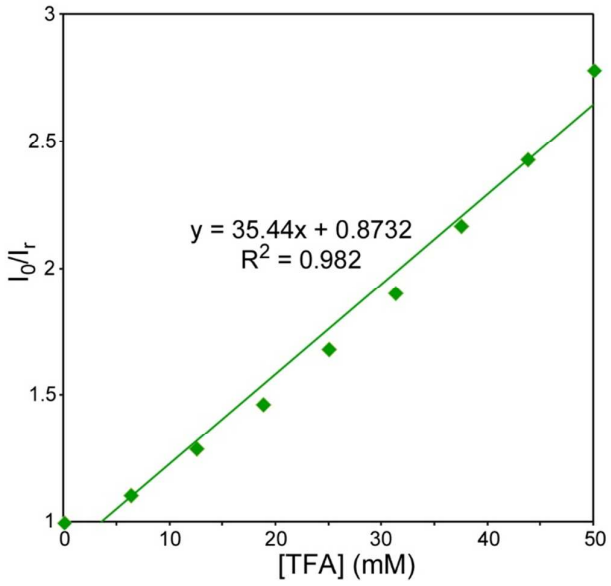

Figure S10. I_0/I_r vs. quencher concentration plot for the emission quenching of **1** by TFA addition in DMF (green). Dots represents experimental I_0/I_r values, solid line represents linear fit to data.

Electronic Properties

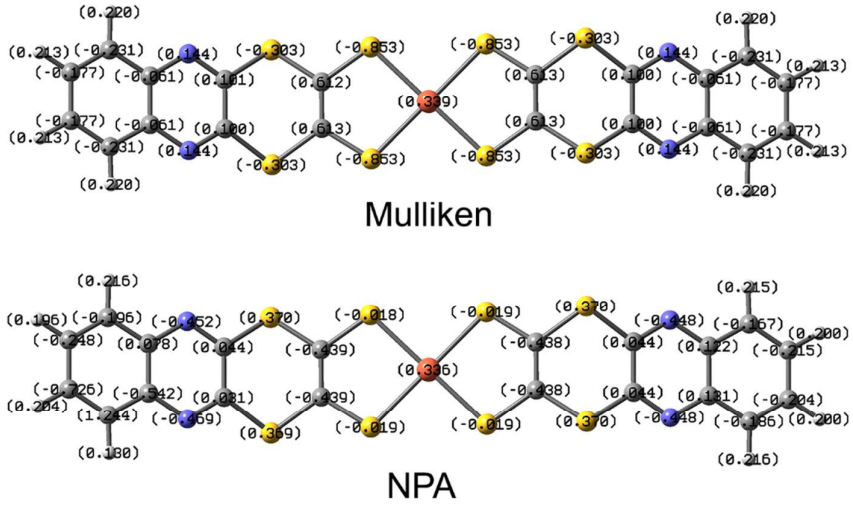

Figure S11.The charge distribution in **1**, obtained by the natural population analysis.

Electrocatalytic activity

Cyclic voltammograms of **1** in CH_3CNsolution acquired upon successive additions of *p*-toluene-sulfonic acid (tosylic acid, TsOH) are reported in Figure S12.The reduction wave relatable to the redox couple $[PtL_2]^-/[PtL_2]^{-2}$ is still observed and new peaks of increasing current on increasing acid concentration and falling at more negative potentials, appear. These peaks are assigned to proton reduction. The cyclic voltammetric responses as a function of added tosylic acid are similar to what observed in analogous nickel radical dithiolenes studied as electrocatalysts for proton reduction.[iv]

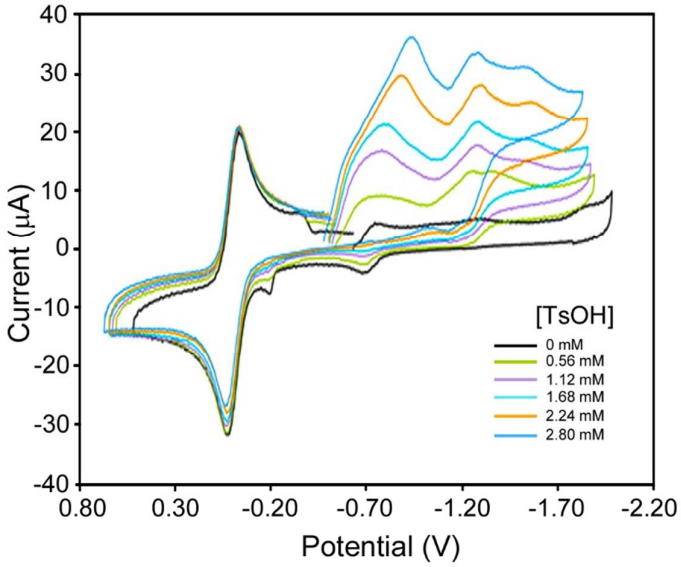

Figure S12. Cyclic voltammograms of **1** [0,65 mM] in CH_3CN solution upon successive additions of TsOH. Working electrode: glassy carbon, GC; Counter electrode: Pt; Reference electrode: Ag; scan rate: 100 mV/s, $TBAClO_4$ 0,2 M, $E_{1/2}(Fc^+/Fc)$ = 0V. All solutions were freshly prepared. Argon was used to purge all samples.

References

i. (a) A. H. Morrish, *The Physical Principles of Magnetism*; IEEE Press: New York, 2001; p. 31. (b) O. Kahn, *Molecular Magnetism*; VCH Publishers: Cambridge, 1993; p. 9

ii. Brouwer, A. M. *Pure Appl. Chem*. **2011**, *83*, 2213.

iii. S. J. Strickler, R. A. J. Berg, *Chem. Phys.***1962**, *37*, 814

iv. Begum, A.; Moula, G.; Sarkar, S. *Chem. Eur. J.* **2010**, *16*, 12324.